NASA TECHNICAL NOTE

NASA TN D-7490

NASA TN D-7490

VELOCITY LAG OF SOLID PARTICLES IN OSCILLATING GASES AND IN GASES PASSING THROUGH NORMAL SHOCK WAVES

by Barry R. Maxwell and Richard G. Seasholtz

Lewis Research Center
Cleveland, Ohio 44135

NATIONAL AERONAUTICS AND SPACE ADMINISTRATION • WASHINGTON, D. C. • MARCH 1974

1. Report No.	2. Government Accession No.	3. Recipient's Catalog No.
NASA TN D-7490		

4. Title and Subtitle	5. Report Date
VELOCITY LAG OF SOLID PARTICLES IN OSCILLATING GASES AND IN GASES PASSING THROUGH NORMAL SHOCK WAVES	March 1974
	6. Performing Organization Code

7. Author(s)	8. Performing Organization Report No.
Barry R. Maxwell, Bucknell University, Lewisburg, Pennsylvania; and Richard G. Seasholtz, Lewis Research Center	E-7653
	10. Work Unit No. 501-24

9. Performing Organization Name and Address	11. Contract or Grant No.
Lewis Research Center National Aeronautics and Space Administration Cleveland, Ohio 44135	

12. Sponsoring Agency Name and Address	13. Type of Report and Period Covered
National Aeronautics and Space Administration Washington, D.C. 20546	Technical Note
	14. Sponsoring Agency Code

15. Supplementary Notes

16. Abstract

The velocity lag of micrometer size spherical particles is theoretically determined for gas-particle mixtures passing through a stationary normal shock wave and also for particles embedded in an oscillating gas flow. The particle sizes (0.125 to 2μm rad) and densities (0.5 to 3 g/cm^3) chosen are those considered important for laser Doppler velocimeter (LDV) applications. The governing equations for each flow system are formulated. The deviation from Stokes flow caused by inertial, compressibility, and rarefaction effects is accounted for in both flow systems by use of an empirical drag coefficient. Graphical results are presented which characterize particle tracking as a function of system parameters.

17. Key Words (Suggested by Author(s))	18. Distribution Statement
Laser-Doppler velocimeter Particle motion Multiphase flow Particle tracking	Unclassified - unlimited Cat. 12

19. Security Classif. (of this report)	20. Security Classif. (of this page)	21. No. of Pages	22. Price*
Unclassified	Unclassified	29	

* For sale by the National Technical Information Service, Springfield, Virginia 22151

VELOCITY LAG OF SOLID PARTICLES IN OSCILLATING GASES AN IN GASES PASSING THROUGH NORMAL SHOCK WAVES

by Barry R. Maxwell* and Richard G. Seasholtz

Lewis Research Center

SUMMARY

The velocity lag of micrometer size spherical particles is theoretically determined for gas-particle mixtures passing through a stationary normal shock wave and also for particles embedded in an oscillating gas flow. The particle sizes (0.125 to 2μm radius) and densities (0.5 to 3 g/cm^3) chosen are those considered important for laser-Doppler velocimeter (LDV) applications. The governing equations for each flow system are formulated. The deviation from Stokes flow caused by inertial, compressibility, and rarefaction effects is accounted for in both flow systems by use of an empirical drag coefficient. In the shock wave study the effects of particle mass loading and convective heat transfer are included. The graphical results presented characterize particle tracking as a function of system parameters.

INTRODUCTION

Laser-Doppler velocimetry (LDV) is an optical technique for determining the velocity of flowing fluids by measuring the velocity of tracer particles entrained in the gas rather than by measuring the velocity of the gas molecules themselves. The LDV technique is of considerable importance in gas dynamic measurements because it is unnecessary to introduce hardware into the flow system. Therefore, problems associated with mounting conventional probes, their disturbance to the flow field and their thermal destruction by hot gases are eliminated.

Since the LDV system measures only the motion of small tracer particles carried by the gas, the accuracy is limited by the accuracy with which the particles follow the gas flow. Therefore, it is important to know how accurately the particles track the gas flow,

*Assistant Professor of Mechanical Engineering, Bucknell University, Lewisburg, Pennsylvania.

and careful consideration must be given to the motion of the particles relative to the carrier gas.

The objective of this study is to determine the velocity lag of spherical particles with sizes (0.125 to 2μm rad) and densities (0.5 to 3 g/cm^3) that are of particular interest in LDV applications. Previous studies of particle tracking for LDV applications have either been restricted to creeping flow (refs. 1 and 2), or to a limited range of system parameters (ref. 3). Other studies (refs. 4 and 5) of gas-particle flows have been conducted, but the results do not generally cover the range of parameters of interest for LDV work.

Two flow systems are analyzed and the velocity lag of the particles relative to the gas is determined as a function of the system parameters. The first flow system is a gas-particle mixture passing through a normal shock wave. The analysis examines the velocity and temperature lags between the gas and particles in the relaxation region behind the shock disturbance. Temperature lags are explored because of the changing temperatures downstream from the shock wave and the effect of such changes on the dynamic behavior of the gas and particles. The second system examined is an oscillating gas-particle flow. The analysis determines the particle velocity lag as a function of particle properties and the amplitude and frequency of the carrier gas oscillations. The response of a particle to an oscillating flow as a function of frequency is useful in determining the limitations of LDV in turbulence measurements.

The research approach of this study is (1) to define the assumptions regarding the gas-particle system, (2) to formulate the equations governing the behavior of the fluid systems, and (3) to define the significant system parameters and conduct a parametric study to determine the response of the systems to their variation. Subsequent sections of this report discuss these items in detail and report the results and conclusions obtained.

ANALYSIS

Simplifying Assumptions

The simplifying assumptions of this study are

(1) The state of the carrier gas is described by the perfect gas law.

(2) The particles are spherical, noninteracting, and uniformly distributed within the carrier gas.

(3) Thermal (Brownian) motion of the particles does not contribute to the system pressure, implying that the number of particles per unit volume is small compared with the number of molecules.

(4) Particle mass transfer by evaporation or condensation is excluded from consideration.

(5) The total energy content of the two-phase system is constant, and the dissipative term in the conservation of energy equation is neglected.

(6) The flow systems are not influenced by solid boundaries.

(7) Each particle, because of its small size, is characterized by uniform temperature.

(8) The particles thermally track the gas phase of the oscillating flow system.

(9) Flow through the shock flow system is steady and one-dimensional.

(10) Viscous effects are neglected except in gas-particle interactions.

(11) The volume occupied by the particles is neglected when calculating state properties of the gas.

These assumptions are used to formulate the basic equations governing the behavior of the gas-particle flow in both flow systems and are regarded as valid for most LDV applications employing naturally occurring or artificially injected contaminants.

Governing Equations

The equations governing the kinematic and thermal behavior of a gas-particle system are the equation of state and the laws of conservation of mass, momentum, and energy of the system. These equations are formulated in a manner consistent with the previous governing assumptions. Definition of symbols is included in the appendix. The equation of state is

$$P = \rho_g RT \tag{1}$$

where P, ρ, R and T denote pressure, mass density, gas constant, and temperature, respectively. The subscript g denotes the gas phase. The conservation of mass for the gas phase and the particles is

$$\dot{m}_g = \rho_g u_g = \text{constant} \tag{2}$$

and

$$\dot{m}_p = \rho_s u_p = \text{constant} \tag{3}$$

where $\dot{m}$ and u denote mass flux and velocity, respectively, and ρ_s is the particle mass per unit volume of gas given by

$$\rho_s = \frac{4}{3}\pi r^3 n_p \rho_p$$

where n_p is the particle number density. Conservation of momentum for the gas-particle mixture is given by

$$\rho_g u_g \frac{du_g}{dx} + \rho_s u_p \frac{du_p}{dx} + \frac{dP}{dx} = 0 \tag{4}$$

and is obtained by combining the momentum equations for the particles and gas phase, thus eliminating the common interaction term. The first and third terms are due to the gas phase, and the second term is attributed to the presence of the particles.

The equation of motion for a single spherical particle in a fluid without external force fields is given in reference 6 as

$$m_p \frac{du_p}{dt} = C_D \rho_g \frac{A}{2} (u_g - u_p)^2 - \frac{m'}{\rho_g} \frac{dP}{dx} - \frac{m'}{2} \left(\frac{du_p}{dt} - \frac{du_g}{dt} \right) + 6r^2 (\pi \mu \rho_g)^{1/2} \int_{t_0}^{t} d\tau \frac{\left(\frac{du_g}{d\tau} - \frac{du_p}{d\tau} \right)}{(t - \tau)^{1/2}} \tag{5}$$

where

$$m_p = 4\pi r^3 \frac{\rho_p}{3}$$

$$m' = 4\pi r^3 \frac{\rho_g}{3}$$

$$\frac{dP}{dx} = \frac{-\rho_g du_g}{dt}$$

and C_D, μ, r, and A denote the viscous drag coefficient, viscosity, particle radius, and cross sectional area, respectively. Equation (5) has been used for creeping flow in several previous particle flow studies (refs. 1 and 2). This equation equates the force to accelerate a particle to the following fluid effects in order of their appearance in the equation.

(1) The viscous drag on the particle expressed in terms of an empirically determined drag coefficient C_D

(2) The force on the particle due to the pressure gradient in the surrounding fluid

(3) The force required to accelerate the mass of fluid which surrounds the particle and moves with it (This term is commonly referred to as the apparent mass term and is viewed as an addition to the inertia of the particle, the increment being one-half (ref. 7) the mass of the fluid displaced.)

(4) The Basset history integral (Basset force, ref. 8), which accounts for the deviation of the flow from steady state and becomes substantial when the particle

is accelerated at a high rate

Conservation of energy for the gas-particle mixture as a whole, thus eliminating interaction terms, is given by

$$\rho_g u_g \left(c_g \frac{dT_g}{dx} + u_g \frac{du_g}{dx} \right) + \rho_s u_p \left(c_s \frac{dT_p}{dx} + u_p \frac{du_p}{dx} \right) = 0 \tag{6}$$

where c_s and c_g denote particle and gas specific heats, respectively. An energy balance on a particle yields

$$u_p \frac{dT_p}{dx} = \frac{3}{2} \frac{Nu\, k_g}{\rho_p c_s r^2} (T_g - T_p) \tag{7}$$

where k_g is the gas thermal conductivity and Nu is an empirically determined Nusselt number defined as $Nu = 2rh/k_g$ (where h is the convective heat transfer coefficient). Equation (7) considers convection heat transfer only since particle temperatures are sufficiently low to preclude significant radiation heat loss.

Shock Wave Flow System

Consider a homogeneous mixture of a gas and particles that passes through a stationary normal shock wave. It is assumed that the gas-particle mixture is in velocity and thermal equilibrium upstream of the shock disturbance. As the mixture passes through the shock, the gas experiences a compression and a velocity decrease consistent with normal gas-dynamic shock relations. Because the particles are large relative to molecular dimensions, they are unable to accommodate themselves to the decreased velocity and increased temperature of the gas immediately downstream from the shock. Therefore, a relaxation zone of finite length exists behind the shock during which momentum and energy exchange cause a gradual reestablishment of thermal and kinematic equilibrium between the phases. Typical velocity and temperature distributions (ref. 4) of the gas-particle mixture are shown qualitatively in figure 1. The velocity and temperature relaxation zones are characterized by the relaxation lengths λ_v and λ_T. These lengths are defined as the distances at which the appropriate particle properties approach to within 1 percent of the corresponding gas properties and are functions of the gas-dynamic and thermophysical properties of the gas-particle system. The intent of this portion of the study is to investigate the extent of the relaxation, or equilibration, zone and to determine how it varies as a function of system properties. Knowledge of the length of the velocity equilibration zone is important for LDV applications downstream of a known shock disturbance because of the velocity lag of tracer particles within this

zone. Conversely, measurement of the relaxation length may be used to determine particle sizes if the properties of the shock are known.

It is convenient to introduce the following dimensionless variables, where the subscript 1 denotes conditions upstream of the shock, the subscript 2 conditions immediately downstream, and the subscript 3 conditions far downstream, where velocity and thermal equilibrium are achieved:

$$\overline{T}_g = \frac{T_g}{T_1} \qquad \overline{u}_g = \frac{u_g}{a_1} \qquad \alpha = \frac{\dot{m}_p}{\dot{m}_g} \qquad M_1 = \frac{u_1}{a_1}$$

$$\overline{T}_p = \frac{T_p}{T_1} \qquad \overline{u}_p = \frac{u_p}{a_1} \qquad \beta = \frac{c_s}{c_g}$$

where a denotes the sonic velocity and α represents the particle mass loading ratio. Equations describing the velocity and temperature distributions in the relaxation zone are obtained by introducing these variables into governing equations (1) to (7).

An equation for the particle velocity variation downstream of the shock is obtained from equation (5) by neglecting the pressure gradient, apparent mass, and Basset integral terms. This simplification is justified in steady-state gas-dynamic flows whose properties are changing very gradually or when the particle mass density is much larger than the gas density (ref. 1). Therefore, equation (5) reduces to

$$\frac{d\overline{u}_p}{dx} = \frac{3}{8}\left(\frac{C_D}{r\overline{u}_p}\right)\left(\frac{\rho_g}{\rho_p}\right)(\overline{u}_g - \overline{u}_p)^2 \tag{8}$$

The equation for the particle temperature variation is obtained from equation (7) and is

$$\frac{d\overline{T}_p}{dx} = \frac{3}{2}\frac{Nu\, k_g}{\rho_p c_s \overline{u}_p r^2 a_1}\left(\overline{T}_g - \overline{T}_p\right) \tag{9}$$

An equation for $d\overline{T}_g/dx$ is obtained by writing the equation of state for the gas (eq. (1)) in terms of the dimensionless variables and differentiating with respect to x to obtain

$$\frac{dP}{dx} = P_1 \frac{M_1}{\overline{u}_g}\left(\frac{d\overline{T}_g}{dx} - \frac{\overline{T}_g}{\overline{u}_g}\frac{d\overline{u}_g}{dx}\right) \tag{10}$$

Substituting this expression for dP/dx into equation (4) yields

$$\frac{d\overline{T}_g}{dx} = \left(\frac{\overline{T}_g}{\bar{u}_g} - \gamma\bar{u}_g\right)\frac{d\bar{u}_g}{dx} - \alpha\gamma\bar{u}_g\frac{d\bar{u}_p}{dx} \tag{11}$$

where γ denotes the ratio of specific heats for the gas phase. To obtain an equation for du_g/dx equation (11) is used to eliminate $d\overline{T}_g/dx$ from equation (6) giving

$$\frac{d\bar{u}_g}{dx} = \frac{\left[\alpha\gamma\bar{u}_g - \alpha(\gamma - 1)\bar{u}_p\right]\frac{d\bar{u}_p}{dx} - \alpha\beta\frac{d\overline{T}_p}{dx}}{\left(\frac{\overline{T}_g}{\bar{u}_g} - \bar{u}_g\right)} \tag{12}$$

where the relations $a_1^2 = \gamma RT_1$ and $\gamma R = c_g(\gamma - 1)$ have been used. Equations (8), (9), (11), and (12) constitute a system of coupled, first-order, nonlinear ordinary differential equations whose simultaneous solution yields the variation of $\bar{u}_g$, $\bar{u}_p$, $\overline{T}_g$, and $\overline{T}_p$ as a function of stream-length x.

The starting conditions for the gas phase are the conditions immediately behind the shock and are provided by the Rankine-Hugoniot (ref. 9) equations for a shock in the gas phase alone. Accordingly,

$$\overline{T}_g(0) = \frac{T_2}{T_1} = \frac{1}{M_1^2}\left[\epsilon^2\left(M_1^2 - 1\right) + M_1^2\right]\left[\epsilon^2\left(M_1^2 - 1\right) + 1\right] \tag{13}$$

$$\bar{u}_g(0) = \frac{u_2}{a_1} = \left\{\frac{T_2}{T_1}\left[\frac{(\gamma - 1)M_1^2 + 2}{2\gamma M_1^2 - (\gamma - 1)}\right]\right\}^{1/2} \tag{14}$$

where $\epsilon^2 = (\gamma - 1)/(\gamma + 1)$. Since the particles pass through the shock without change in their velocity and temperature, the particle phase starting conditions are

$$\overline{T}_p(0) = 1 \tag{15}$$

$$\bar{u}_p(0) = M_1 \tag{16}$$

Oscillating Flow System

Consider a gas-particle system in which the gas is undergoing periodic velocity fluctuations characterized by a constant amplitude and a single fixed frequency. Because the size and mass of the particles are large relative to molecular quantities, the particles are unable to track the gas for all flow conditions, and a phase and velocity lag develops between the particles and the carrier gas. Particle tracking may be characterized by the amplitude ratio $(u_p)_{max}/u_o$ where $(u_p)_{max}$ and u_o denote the maximum velocities attained by the particles and gas, respectively, in the oscillating flow system. It is of interest to examine the sensitivity of this amplitude ratio to the frequency and amplitude of oscillation and to the system thermophysical properties.

Although no real flow system is characterized by oscillations at a single fixed frequency, it is important to understand the behavior of such a system in order to effectively analyze a turbulent flow system oscillating over a broad spectrum of frequencies.

The general equation of motion of a particle in a fluid is given by equation (5), and the oscillating flow field is described by

$$u_g = u_o \sin 2\pi ft \tag{17}$$

where f and t denote frequency and time. For purposes of this study the apparent mass term and the pressure gradient term of equation (5) are retained, but the Basset history integral term in neglected. Deletion of the Basset force is justified (refs. 1 and 2) for flow systems with the range of particle-to-gas density ratios and frequencies encountered in this study. Introducing equation (17) into equation (5), deleting the Basset integral, and simplifying yield

$$\frac{du_p}{dt} = \frac{C_D \rho_g \frac{A}{2} (u_o \sin \omega t - u_p)^2 + \frac{3}{2} m' \omega u_o \cos \omega t}{m_p + \frac{m'}{2}} \tag{18}$$

where $\omega = 2\pi f$. Equation (18) is a nonlinear ordinary differential equation whose solution yields the variation of u_p as a function of time. The initial condition is $u_p(0) = 0$. Equation (18) is numerically integrated for several conditions of physical interest which are subsequently defined in the Parametric Study section of this report.

Empirical Drag and Heat Transfer Laws

The rate of momentum and energy transfer between phases of a two-phase flow

system is fundamental to the understanding and analysis of such a system and is typically characterized in terms of a drag coefficient and Nusselt number. In general, C_D and Nu depend on particle geometry, Reynolds number, Mach number, and Knudsen number. There has been some theoretical work and a great deal of experimental work conducted to determine the appropriate functional dependence on these parameters, but the literature often indicates a wide discrepancy in the reported results.

In the absence of reliable drag data, the drag coefficient is frequently assumed to be given by the classical Stokes drag law

$$C_D = \frac{24}{Re} \tag{19}$$

where $Re = 2r\rho_g(u_g - u_p)/\mu$ is the Reynolds number. The Nusselt number is usually approximated by an expression obtained by Knudsen and Katz (ref. 10) for flow around a single sphere:

$$Nu = 2 + 0.6\ Pr^{1/3}Re^{1/2} \tag{20}$$

where $Pr = \mu c_g/k_g$ is the gas phase Prandtl number.

Although it is most convenient to use Stokes law for the drag coefficient, it becomes increasingly unrealistic for Reynolds numbers above approximately 1.0 and in flows where rarefaction and inertial effects are significant. When conditions are known to deviate from Stokes flow, investigators have used various empirically determined drag coefficients to account for the deviation. Since differences appear in the literature regarding the most appropriate drag coefficient for a given flow system, any momentum exchange analysis is only as valid as the drag coefficient employed. Differences are generally attributed to such phenomena as rarefaction, compressibility, acceleration, electrostatic charge effects, unsteady nature of the flow, etc.

Probstein and Fassio (ref. 11) present an empirical drag expression which approximates the standard drag curve for a sphere:

$$C_D = aRe^{-n} \tag{21}$$

where for $Re < 1$

$$a = 24 \quad \text{and} \quad n = 1$$

for $1 < Re < 10^3$

$$a = 24 \text{ and } n = \frac{3}{5}$$

and for $Re > 10^3$

$$a = 0.44 \quad \text{and} \quad n = 0$$

Alternate empirical expressions frequently used by investigators are (refs. 3 and 12)

$$C_D = 0.48 + 28\ Re^{-0.85} \tag{22}$$

and (ref. 13)

$$C_D = 27\ Re^{-0.84} \tag{23}$$

The gas-dynamic flow regimes frequently encountered by micrometer size particles require appropriate corrections to account for inertial, rarefaction, and compressibility effects. Carlson and Hoglund (ref. 14) present a drag expression that corrects the Stokes law for these effects and is, therefore, usable throughout the continuum, slip and transition regimes. The expression is

$$C_D = \frac{24}{Re} \left\{ \frac{(1 + 0.15\ Re^{0.687}) \left[1 + \exp\left(\frac{-0.427}{M^{4.63}} - \frac{3}{Re^{0.88}} \right) \right]}{1 + \frac{M}{Re} \left[3.82 + 1.28 \exp \frac{(-1.25\ Re)}{M} \right]} \right\} \tag{24}$$

where the term in the bracket accounts for deviation from Stokes flow caused by inertial, compressibility, and rarefaction effects.

Equations (24) and (20) are used in this study for the drag coefficient and Nusselt number. This selection is based on their broad range of applicability and their wide acceptance in the literature. However, in order to assess the sensitivity of the flow system to variations in drag coefficient assumptions, several calculations are performed where the only variable is the drag law. Results of this analysis are discussed later in this report.

PARAMETRIC STUDY

When analyzing any gas-particle flow system, the relations between the many variables involved are complicated, and the consequences of varying the system properties are not readily apparent. In order to understand the behavior of both the shock flow system and the oscillating flow system, the significant parameters that influence each system are defined and then systematically varied over ranges of interest for LDV

applications. The limits of the parametric study are specified below for each flow system.

Shock Wave Flow System

The behavior of the shock flow system is governed by equations (8), (9), (11), and (12). The parameters that influence the system are the Mach number M_1, specific heat ratio β, particle radius r, mass density ρ_p, and mass loading α. The influence of these parameters on the relaxation zone structure is explored by numerically integrating the governing equations while varying each parameter and holding the remaining ones constant. The cases examined and the corresponding values of the parameters are summarized in table I. The range of values investigated for each of the parameters was selected in order to correspond to typical values encountered in most LDV applications (refs. 15 and 16). Particle mass loading ratios of $\alpha = 0$ and $\alpha = 0.2$ were chosen to represent the extremes of negligible and heavy particle mass fractions. Momentum and energy exchange are characterized by equations (24) and (20), respectively, and initial gas pressure and temperature are 1 atmosphere and 289 K (520° R).

In addition, the sensitivity of the system to a change in empirical drag law is investigated by fixing the parameters in table I and using equations (19) and (21) to (24) separately to characterize the momentum exchange.

Oscillating Flow System

The parameters that directly influence the oscillating system are particle radius, mass density, and the amplitude and frequency of gas oscillation. The range of values considered in this study is summarized in table II.

Equation (18) is numerically integrated for each condition defined in table II, and the results are graphically summarized later in this report. The gas pressure and temperature are fixed at 1 atmosphere and 289 K (520° R), respectively, and the drag coefficient is given by equation (24).

RESULTS

Shock Wave System

The results of numerically integrating equations (8), (9), (11), and (12) with the input values summarized in table I are presented in figures 2 to 8.

Figure 2 demonstrates the typical structure of the relaxation zone in nondimen-

sionalized form. The decrease of gas velocity in the equilibration region is attributed to the positive temperature gradient of the particles. The thermal influence of the particles on the gas velocity is observed in equation (12). Although the structure is plotted for a particle radius of 1 micrometer and a density of 1 gram per cubic centimeter, it was found that this nondimensionalized structure is displayed (within 1 percent) for all other radii and densities examined in cases 1 and 2 (table I) when $\alpha = 0.2$. When $\alpha = 0$ there is a negligible number of particles present in the flow to alter the dynamic and thermal behavior of the gas, and, as equations (12) and (11) indicate, the gas velocity and temperature are equal to the values dictated by equations (14) and (13) throughout the equilibration zone.

The influence of particle radius and mass density on the velocity and thermal relaxation lengths is demonstrated in figures 3 and 4 for particle mass loading ratios of $\alpha = 0$ and $\alpha = 0.2$. The results indicate that an increase in either radius or density results in a significant extension of the relaxation zones and that the relaxation lengths are relatively insensitive to particle loading. Also, the particles equilibrate more rapidly to the gas temperature than to the velocity, thus indicating that energy is transferred more effectively than momentum between the phases.

Figure 5 shows the variation of the relaxation lengths as a function of the particle mass loading ratio and indicates that an increase in mass loading results in a decrease in the relaxation zone lengths. This trend is attributed to the fact that additional energy and momentum are extracted from the gas by the solid particles as their mass fraction increases. The influence of the Mach number on the relaxation lengths is shown in figure 6 for mass loading ratios of $\alpha = 0$ and $\alpha = 0.2$. When the particle mass loading is zero, the relaxation lengths became maximum at approximately Mach 1.3 and then decrease as the Mach number increases. Although not observable in figure 5, the maximum equilibration length for the $\alpha = 0.2$ case would occur below Mach 1.1. The decrease of the relaxation lengths toward zero as the Mach number approaches 1 is a result of the way the relaxation lengths were defined (e.g., when the gas velocity changes less than 1 percent the relaxation lengths are 0).

Figure 7 presents the relaxation lengths as a function of $\beta = c_s/c_g$ for mass loading ratios of $\alpha = 0$ and $\alpha = 0.2$. The results indicate that an increase in β extends both relaxation zones and that the thermal equilibration length is the most sensitive to a change in β. An increase in β results in additional thermal energy required from the gas in order to achieve a given increase in particle temperature. This results in slightly lower values for postshock equilibrium velocity and temperature and in an increase in the equilibration lengths.

Figure 8 compares the relaxation zone structure as a function of different drag law assumptions. The particles respond least rapidly when Stokes flow is assumed, and the response for the various empirical laws is generally similar. It is also evident that the particle velocities for the $\alpha = 0$ case are significantly higher than when particles are

present in the flow. This is due to the fact that when $\alpha = 0$ there are no particles assumed available to extract momentum from the carrier gas. Therefore, the kinetic energy of the gas remains unchanged downstream from the shock (eq. (12)), and the few particles present achieve the highest velocity, consistent with the drag law, throughout the flow field.

Oscillating Flow System

The results of numerically integrating equation (18) for the range of values given in table II are presented in figures 9 to 13.

Figures 9 and 10 represent typical examples of the particle response to the oscillating flow field over a several cycle period. The gas and particles start from rest; the motion of the gas is described by equation (17) and $(u_p/u_o)_{max}$ is determined after apparent equilibrium is reached in the particle oscillation.

Figure 11 demonstrates the effect of particle radius on particle trackability. It is seen that frequency response for small particles (0.5 μm or less) is quite good out to a frequency of 10 kilohertz but falls off at higher frequencies. As expected, particle tracking is significantly decreased as particle size increases.

The effect of particle mass density on particle response is presented in figure 12. At high frequencies an increase in particle density causes a significant decrease in particle tracking; at lower frequencies, tracking is less sensitive to a density increase.

Figure 13 shows the effect of gas velocity amplitude on particle response, and it is seen that particle tracking is sensitive to velocity amplitude at frequencies above 10 kilohertz. Because of an increase in the drag coefficient, an increase in u_o results in reduced velocity lag at high frequencies and, therefore, better particle tracking.

CONCLUSIONS

The numerically obtained results of this study provide justification for the following conclusions:

1. The relaxation zone behind a normal shock wave is lengthened whenever the particle radius or mass density increases or whenever the mass loading ratio or Mach number (for $M_1 \gtrsim 1.3$) is reduced.

2. Particle size and mass density have negligible effect on the nondimensional velocity and temperature in the normalized equilibration zone when the Mach number and particle mass loading are fixed.

3. For values of the particle-to-gas specific heat ratio less than approximately 1.5, thermal equilibration occurs before velocity equilibration in the shock flow system. But the thermal equilibration length approaches and exceeds the velocity length as the particle specific heat is increased.

4. Particle tracking in an oscillating gas is improved whenever particle size, mass density, or gas frequency is reduced or when the gas velocity amplitude is increased.

The results obtained in this study should provide useful data for establishing guidelines for the application of laser-Doppler techniques to gas-dynamic velocity measurements.

Lewis Research Center,
National Aeronautics and Space Administration,
Cleveland, Ohio, November 11, 1973,
501-24.

APPENDIX - SYMBOLS

A	particle cross-sectional area, m^2
a	sonic speed, m/sec
C_D	drag coefficient
c_g	gas specific heat at constant pressure, J/kg·K
c_s	particle specific heat, J/kg·K
f	gas frequency, Hz
h	convective heat transfer coefficient, $J/hr \cdot m^2 \cdot K$
k_g	gas thermal conductivity, J/hr·m·K
M	Mach number
$\dot{m}$	mass flow rate, $kg/sec \cdot m^2$
Nu	Nusselt number, $= 2rh/k_g$
n_p	particle number density, $particles/m^3$
P	pressure, N/m^2
Pr	Prandtl number, $= \mu c_g/k_g$
R	gas constant, J/kg·k
Re	Reynolds number, $2r\rho u/\mu$
r	particle radius, meters
T	temperature, K
$\overline{T}$	dimensionless temperature $= T/T_1$
t	time, sec
u	velocity, m/sec
$\overline{u}$	dimensionless velocity $= u/u_1$
x	distance, m
α	particle mass loading ratio, $\dot{m}_p/\dot{m}_g$
β	ratio of particle to gas specific heats, c_s/c_g
γ	ratio of specific heats for gas phase

λ_T temperature relaxation length, m, distance corresponding to point where T_p approaches to within 1 percent of T_g

λ_v velocity relaxation length, m, distance corresponding to point where u_p approaches to within 1 percent of u_g

μ viscosity, $N \cdot sec/m^2$

ρ mass density, kg/m^3

ρ_s particle mass per unit volume of gas

ω angular velocity, rad/sec

Subscripts:

g gas

p particles

1 upstream from shock

2 immediately downstream from shock

REFERENCES

1. Hjelmfelt, A. T., Jr.; and Mockros, L. F.: Motion of Discrete Particles in a Turbulent Fluid. Appl. Sci. Res., vol. 16, 1966, pp. 149-161.

2. Karchmer, Allen M.: Particle Trackability Considerations for Laser Doppler Velocimetry. NASA TM X-2628, 1972.

3. Yanta, William J.; Gates, David F.; and Brown, Francis W.: The Use of a Laser Doppler Velocimeter in Supersonic Flow. Rep. NOLTR-71-169, Naval Ordnance Laboratory (AD-737202), Aug. 25, 1971.

4. Rudinger, G.: Some Properties of Shock Relaxation in Gas Flows Carrying Small Particles. Phys. Fluids, vol. 7, no. 5, May 1964, pp. 658-662.

5. Marble, F. E.: Dynamics of a Gas Containing Small Solid Particles. Fifth AGARD Combustion and Propulsion Colloquium. Pergamon Press, 1963, pp. 175-213.

6. Soo, S. L.: Fluid Dynamics of Multiphase Systems. Blaisdell Publ. Co., 1967.

7. Lamb, Horace: Hydrodynamics. Sixth ed., Dover Publications, 1932, p. 124.

8. Basset, A. B.: A Treatise on Hydrodynamics. Vol. 2. Dover Publications, 1961, p. 291.

9. Ames Research Staff: Equations, Tables, and Charts for Compressible Flow. NACA Rep. 1135, 1953.

10. Knudsen, James G.; and Katz, Donald L.: Fluid Mechanics and Heat Transfer. McGraw-Hill Book Co., Inc., 1958, p. 511.

11. Probstein, Ronald F.; and Fassio, Franco: Dusty Hypersonic Flows. AIAA J., vol. 8, no. 4, Apr. 1970, pp. 772-779.

12. Gilbert, Mitchell; David, Leo; and Altman, David: Velocity Lag of Particles in Linearly Accelerated Combustion Gases. Jet Propulsion, vol. 25, no. 1, Jan. 1955, pp. 26-30.

13. Ingebo, Robert D.: Drag Coefficients for Droplets and Solid Spheres in Clouds Accelerating in Air-Streams. NACA TN 3762, 1956.

14. Carlson, Donald J.; and Hoglund, Richard F.: Particle Drag and Heat Transfer in Rocket Nozzles. AIAA J., vol. 2, no. 11, Nov. 1964, pp. 1980-1984.

15. Fuller, C. E.: Development Testing and Application of a Three-Dimensional Laser Doppler Velocimeter for the Measurement of Gas Flows. Rep. ER-1678 Hayes International Corp. (NASA CR-102948), Apr. 1970.

16. Stevenson, W. H.; and Thompson, H. D.: The Use of the Laser Doppler Velocimeter for Flow Measurements. Purdue Univ. (AD-753243), Nov. 1972.

TABLE I. - SHOCK FLOW PARAMETRIC VALUES

Case	Particle radius, r, μm	Particle density, ρ_p, g/cm^3	Particle mass loading, α	Mach number, M_1	Specific heat ratio, β
1	0.125, 0.25, 0.5, . . . , 1	1	0, 0.2	1.6	1.125
2	0.5	0.5, 1, 1.5, . . . , 3	0, 0.2	1.6	↓
3	↓	1	0, 0.05, 0.1, 0.15, . . . , 1	1.6	
4		1	0, 0.2	1.1, 1.2, . . . , 2	
5		1	0, 0.2	1.6	0.5, 1, . . . , 3

TABLE II. - OSCILLATING FLOW PARAMETRIC VALUES

Case	Particle radius, r, μm	Particle density, ρ_p, g/cm^3	Gas frequency, f, kHz	Gas velocity amplitude, u_1, m/sec (ft/sec)
1	0.125, 0.25, 0.375, 0.5, 0.75, 1, 2	1	0.5 - 128	15.2(50)
2	0.5	0.5, 1, 1.5, . . . , 3	.5 - 128	15.2(50)
3	.5	1	.5 - 128	0.304, 1.52, 15.2, 30.4, . . . , 91.4 (1, 5, 50, 100, . . . , 300)

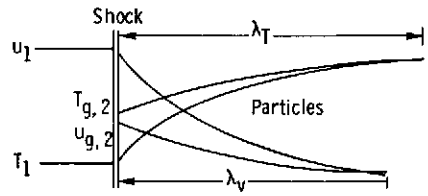

Figure 1. - Qualitative velocity and temperature distributions of gas-particle mixture across normal shock wave.

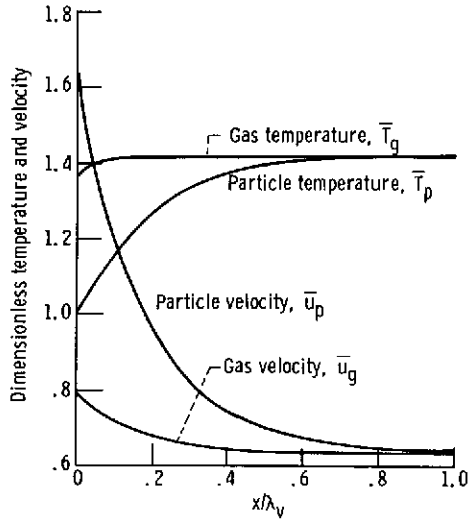

Figure 2. - Dimensionless temperature and velocity distributions behind stationary normal shock wave. Upstream pressure, 1 atmosphere; upstream temperature, 289 K; upstream Mach number, 1.6; particle mass loading ratio, 0.2; ratio of particle to gas specific heats, 1.125; particle mass density, 1 gram per cubic centimeter; particle radius, 1 micrometer.

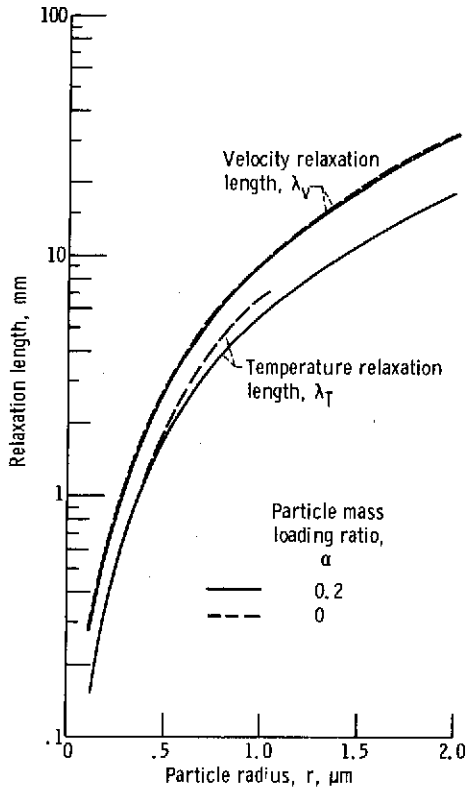

Figure 3. - Shock wave system relaxation lengths as function of particle radius. Upstream pressure, 1 atmosphere; upstream temperature, 289 K; upstream Mach number, 1.6; particle mass density, 1 gram per cubic centimeter.

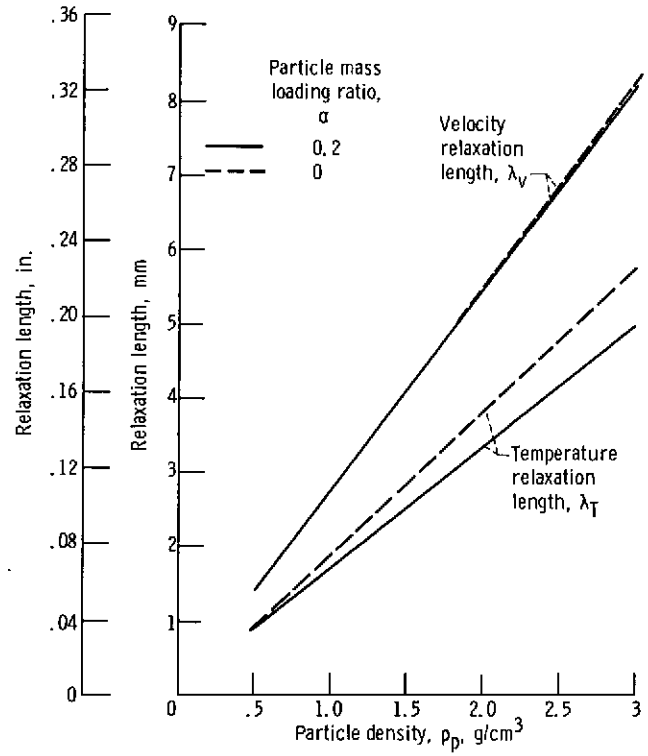

Figure 4. - Shock wave system relaxation lengths as function of particle mass density. Upstream pressure, 1 atmosphere; upstream temperature, 289 K; particle radius, 0.5 micrometer; upstream Mach number, 1.6.

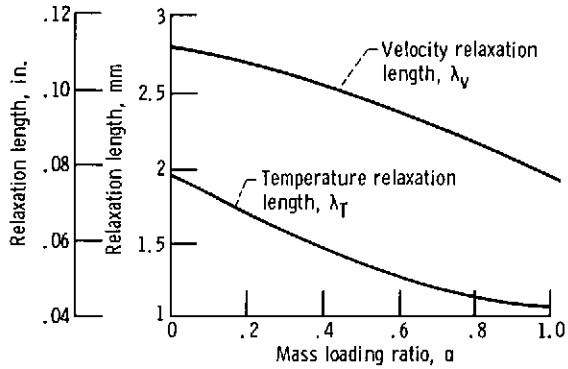

Figure 5. - Shock wave system relaxation lengths as function of particle mass loading ratio. Upstream pressure, 1 atmosphere; upstream temperature, 289 K; upstream Mach number, 1.6; particle radius, 0.5 micrometer; particle mass density, 1 gram per cubic centimeter; ratio of particle to gas specific heats, 1.125.

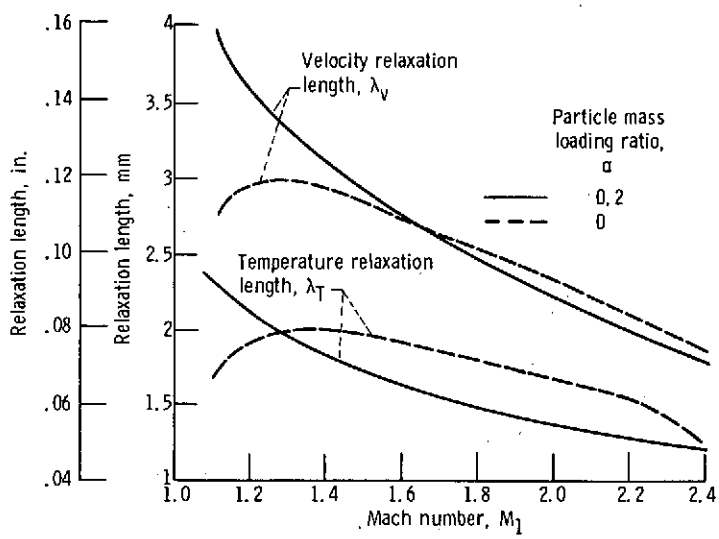

Figure 6. - Shock wave system relaxation lengths as function of Mach number. Upstream pressure, 1 atmosphere; upstream temperature, 289 K; particle density, 1 gram per cubic centimeter; particle radius, 0.5 micrometer.

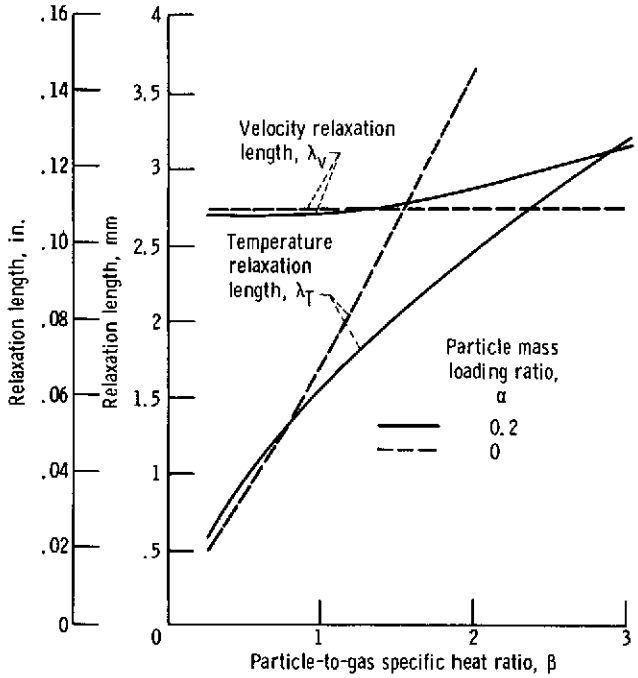

Figure 7. - Shock wave system relaxation lengths as function of particle-to-gas specific heat ratio. Upstream pressure, 1 atmosphere; upstream temperature, 289 K; upstream Mach number, 1.6; particle radius, 0.5 micrometer; particle mass density, 1 gram per cubic centimeter.

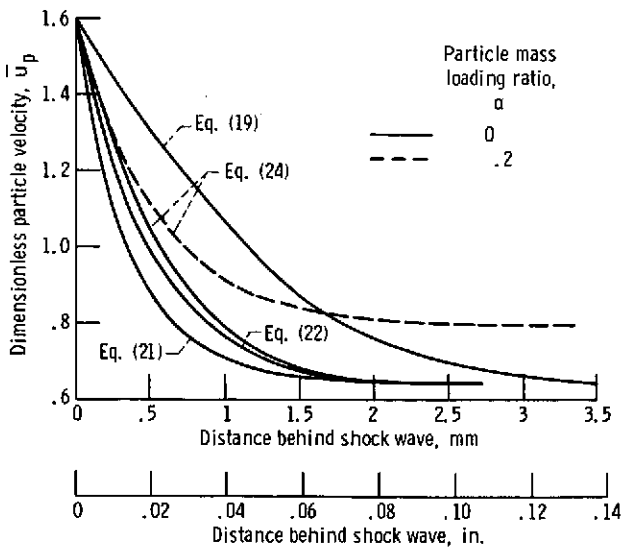

Figure 8. - Influence of drag law on dimensionless velocity distribution behind normal shock wave. Upstream pressure, 1 atmosphere; upstream temperature, 289 K; upstream Mach number, 1.6; particle mass density, 1 gram per cubic centimeter; particle radius, 0.5 micrometer.

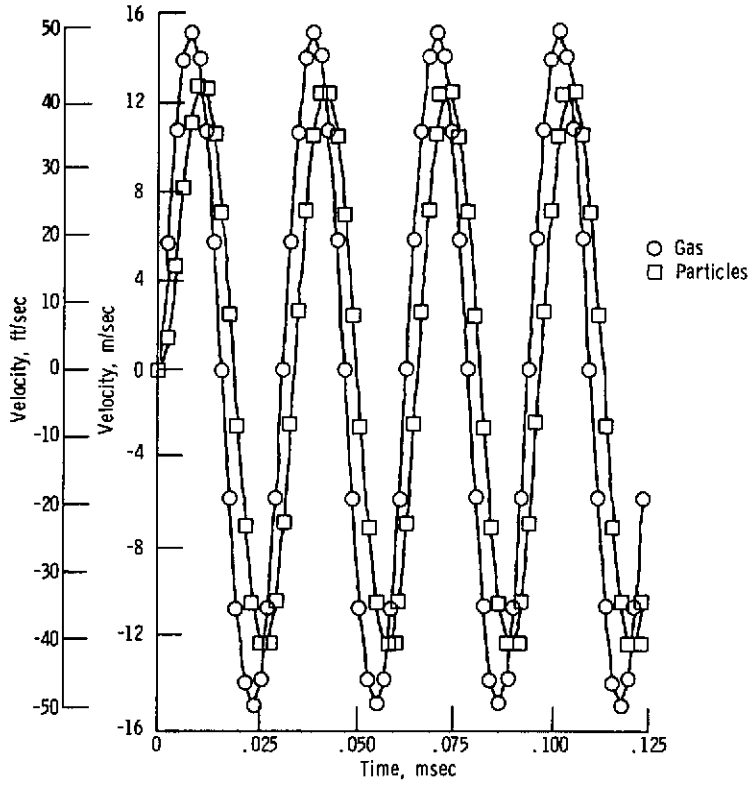

Figure 9. - Particle response to oscillating flow field. Particle radius, 0.5 micrometer; particle mass density, 1 gram per cubic centimeter; maximum gas velocity, 15.2 meters per second; gas frequency, 32 kilohertz.

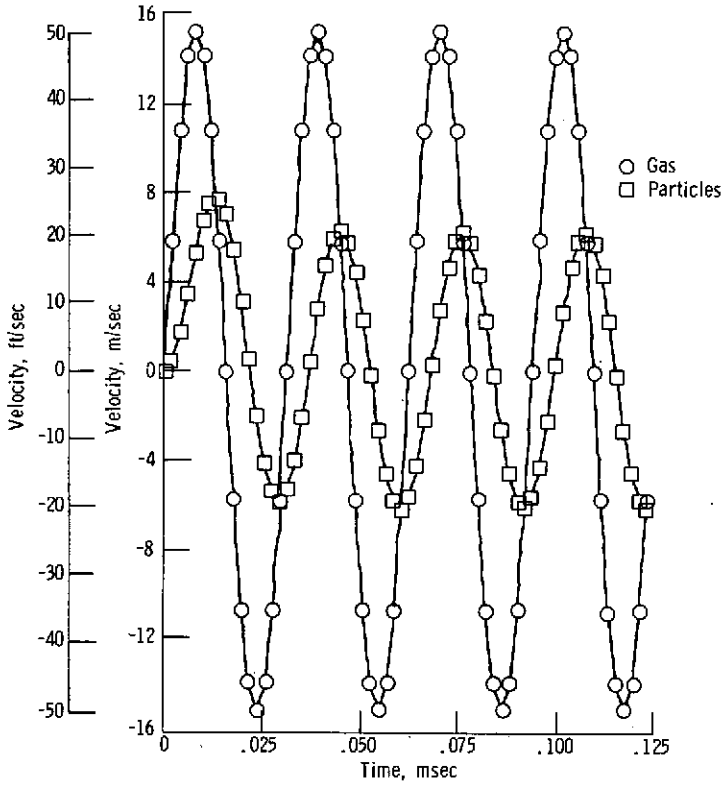

Figure 10. - Particle response to oscillating flow field. Particle radius, 1 micrometer; particle mass density, 1 gram per cubic centimeter; maximum gas velocity, 15.2 meters per second; gas frequency, 32 kilohertz.

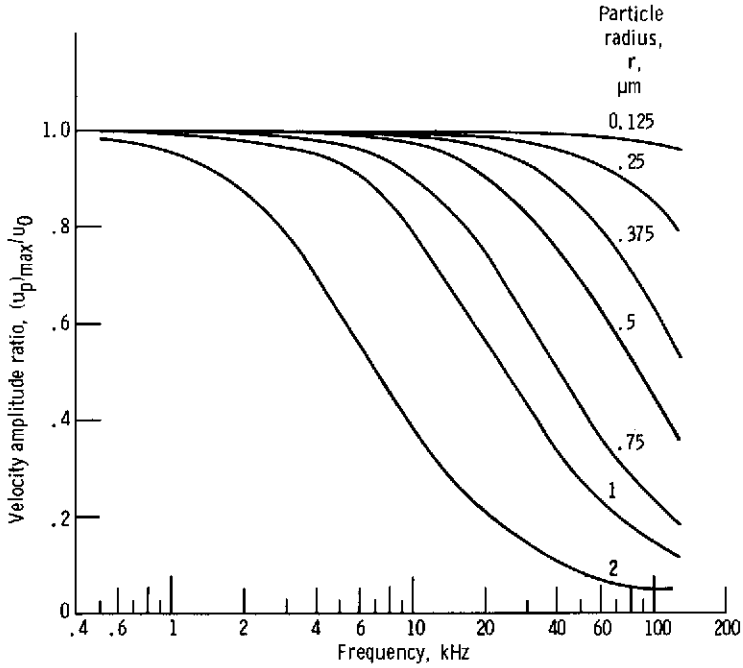

Figure 11. - Influence of particle size on particle tracking in oscillating flow field. Particle mass density, 1 gram per cubic centimeter; maximum gas velocity, 15.2 meters per second.

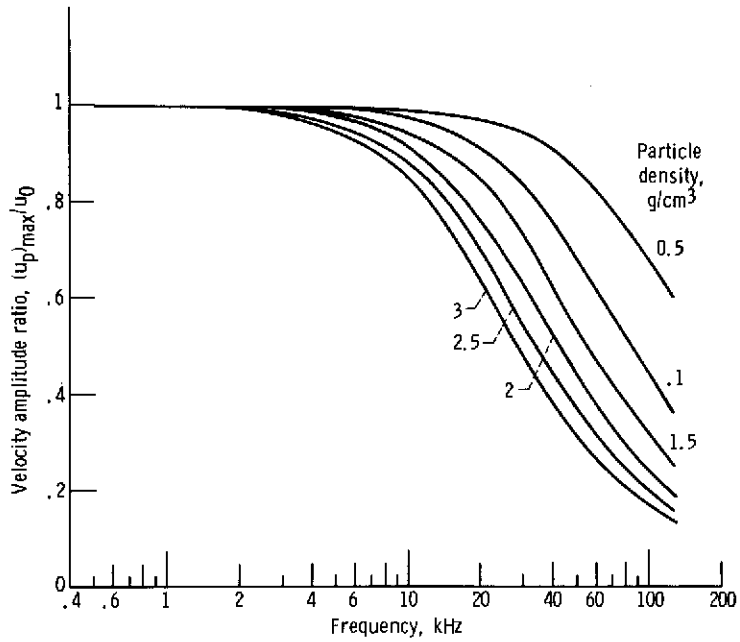

Figure 12. - Influence of particle mass density on particle tracking in an oscillating flow field. Particle radius, 0.5 micrometer; maximum gas velocity, 15.2 meters per second.

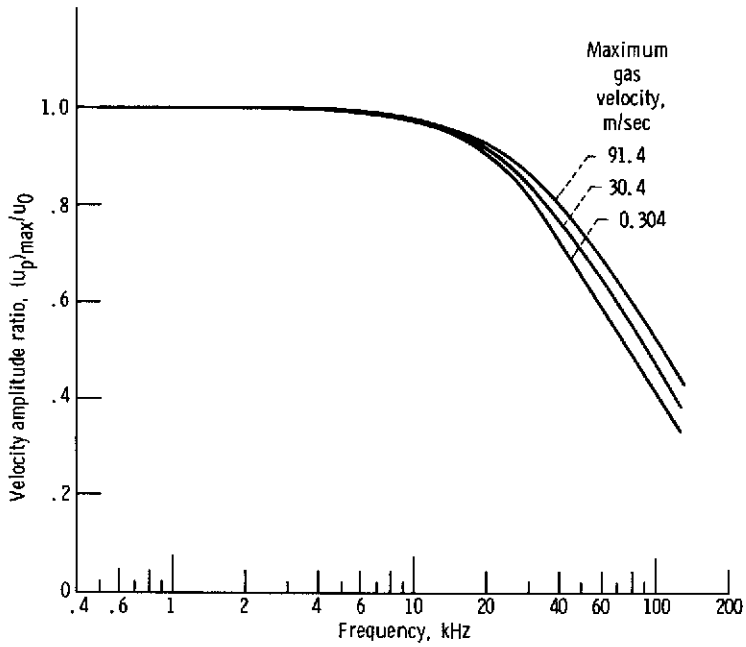

Figure 13. - Influence of maximum gas velocity on particle tracking in an oscillating flow field. Particle radius, 0.5 micrometer; maximum gas velocity, 1 gram per cubic centimeter.

NASA-Langley, 1974 E-7653